

## Structure–Activity Relationship Analysis of Novel Derivatives of Narciclasine (an *Amaryllidaceae* Isocarbostryl Derivative) as Potential Anticancer Agents

Laurent Ingrassia,<sup>†,‡</sup> Florence Lefranc,<sup>†,§,||,∇</sup> Janique Dewelle,<sup>‡</sup> Laurent Pottier,<sup>||</sup> Véronique Mathieu,<sup>||</sup> Sabine Spiegl-Kreinecker,<sup>⊥</sup> Sébastien Sauvage,<sup>‡</sup> Mohamed El Yazidi,<sup>‡</sup> Mischaël Dehoux,<sup>‡</sup> Walter Berger,<sup>#</sup> Eric Van Quaquebeke,<sup>‡</sup> and Robert Kiss<sup>\*,||,∇</sup>

Unibioscreen SA, 40 Avenue Joseph Wybran, 1070 Brussels, Belgium, Service de Neurochirurgie, Cliniques Universitaires de Bruxelles, Hôpital Erasme, Université Libre de Bruxelles, Brussels, Belgium, Laboratoire de Toxicologie, Institut de Pharmacie, Université Libre de Bruxelles, Campus de la Plaine, CP205/1, Boulevard du Triomphe, 1050 Brussels, Belgium, Department of Neurosurgery, Wagner Jauregg Hospital, Linz, Austria, Institute of Cancer Research, Department of Medicine I, Medical University of Vienna, Austria

Received October 27, 2008

Narciclasine (**1**) is a plant growth regulator that has been previously demonstrated to be proapoptotic to cancer cells at high concentrations ( $\geq 1 \mu\text{M}$ ). Data generated in the present study show that narciclasine displays potent antitumor effects in apoptosis-resistant as well as in apoptosis-sensitive cancer cells by impairing the organization of the actin cytoskeleton in cancer cells at concentrations that are not cytotoxic ( $\text{IC}_{50}$  values of 30–90 nM). The current study further revealed that any chemical modification to the narciclasine backbone generally led to compounds of variable stability, weaker activity, or even the complete loss of antiproliferative effects in vitro. However, one hemisynthetic derivative of narciclasine, compound **7k**, demonstrated by both the intravenous and oral routes higher in vivo antitumor activity in human orthotopic glioma models in mice when compared to narciclasine at nontoxic doses. Narciclasine and compound **7k** may therefore be of potential use to combat brain tumors.

### Introduction

About 90% of cancer patients die from their metastases or from the dramatic invasion of vital organs. Gliomas,<sup>1</sup> melanomas,<sup>2</sup> esophageal cancer,<sup>3</sup> pancreatic cancer,<sup>4</sup> hormone refractory prostate cancer,<sup>5</sup> and non-small-cell lung cancers (NSCLC<sup>a</sup>)<sup>6</sup> are among those associated with the most dismal prognoses because of their inherent resistance to apoptosis, especially in their metastatic form. Unfortunately, most of the agents used today by clinicians to combat cancer are pro-apoptotic drugs, which are rather ineffective in combating apoptosis-resistant metastatic cancers.<sup>7</sup> Great hope is therefore being invested in molecules able to kill metastatic or highly invasive cancer cells by nonapoptotic means, notably for example pro-autophagic drugs.<sup>7</sup> Effort is also being made to discover and develop new types of compounds that may be able to selectively decrease the migration of cancer cells, notably metastatic cancer cells, and increase their sensitivity to cytotoxic drugs with either pro-apoptotic and/or pro-autophagic effects.<sup>8–10</sup>

Natural products have played a highly significant role in the discovery and development of new drugs for the treatment of

human diseases.<sup>11,12</sup> This is especially true in the cancer field, where about half the drugs are of natural origin<sup>13,14</sup> and include two of the most important anticancer agents taxol and taxotere.<sup>14</sup> The antitumor potential of *Amaryllidaceae* isocarbostryl derivatives, the most widely known of which are narciclasine (**1**), lycoricidine, and pancratistatin (Figure 1), has long been studied and has been recently reviewed.<sup>15,16</sup> Extracts of *Narcissus* bulbs have been known for millennia from folk medicine for their antitumor effects. The powerful anticancer properties of *Narcissus poeticus* L. were already known to Hippocrates of Kos (ca. 460–370 BCE), who recommended narcissus oil for the treatment of uterine tumors.<sup>16</sup> His successors, the ancient Greek physicians Pedanius Dioscorides (ca. 40–90 AD) and Scranus of Ephesus (98–138 AD), used this therapy to treat various types of cancer.<sup>16</sup> In 1877, a first *Amaryllidaceae* derivative, lycorine, was isolated from *Narcissus pseudonarcissus*<sup>16</sup> and since then more than 100 have been isolated from *Amaryllidaceae* species.<sup>15,16</sup> Kornienko and Evidente<sup>16</sup> reported that it was likely that isocarbostryl constituents of *Amaryllidaceae*, such as narciclasine, pancratistatin, and their congeners, were the most important ingredients responsible for the therapeutic benefits of these plants in the folk medicine treatment of cancer. Narciclasine's (**1**) anticancer activity was evidenced for the first time by Ceriotti et al. in 1967, who described the compound as antimitotic and displaying colchicine-like effects.<sup>17</sup> Narciclasine and pancratistatin also emerged as interesting antitumor drugs in the NCI database.<sup>15</sup> Carrasco et al.<sup>18</sup> reported that narciclasine interacts with the 60S eukaryotic ribosome subunit and inhibits the peptide bond formation step in eukaryotic protein synthesis. More recently, McLachlan et al.<sup>19</sup> demonstrated that pancratistatin, whose chemical structure is very close to that of narciclasine (Figure 1), induces rapid apoptosis in SHSY-5Y neuroblastoma cells. We ourselves recently reported that narciclasine at concentrations  $\geq 1 \mu\text{M}$  appears to induce marked apoptosis-mediated cytotoxic effects in human carcinoma cells but not in normal fibroblasts by activation of the death receptor pathway.<sup>20</sup>

\* To whom correspondence should be addressed. Phone: +32 477 62 20 83. Fax: +32 23 32 53 35. E-mail: rkiss@ulb.ac.be.

<sup>†</sup> The first two authors contributed equally to this work.

<sup>‡</sup> Unibioscreen SA.

<sup>§</sup> Service de Neurochirurgie, Cliniques Universitaires de Bruxelles, Hôpital Erasme, Université Libre de Bruxelles.

<sup>||</sup> Laboratoire de Toxicologie, Institut de Pharmacie, Université Libre de Bruxelles.

<sup>⊥</sup> Department of Neurosurgery, Wagner Jauregg Hospital.

<sup>#</sup> Institute of Cancer Research, Department of Medicine I, Medical University of Vienna.

<sup>∇</sup> R.K. is a Director of Research at the Belgian National Fund for Scientific Research (FNRS, Belgium). F.L. is a Clinical Research Fellow with the FNRS.

<sup>a</sup> Abbreviations: GBM, glioblastoma; HUVEC, human umbilical vein endothelial cell; MOMP, mitochondrial outer membrane permeabilization; NOAEL, no-adverse-effect level; NOEL, no-effect dose level; NSCLC, non-small-cell lung cancer; OMM, outer mitochondrial membrane; SAR, structure–activity relationship; TMZ: temozolomide.

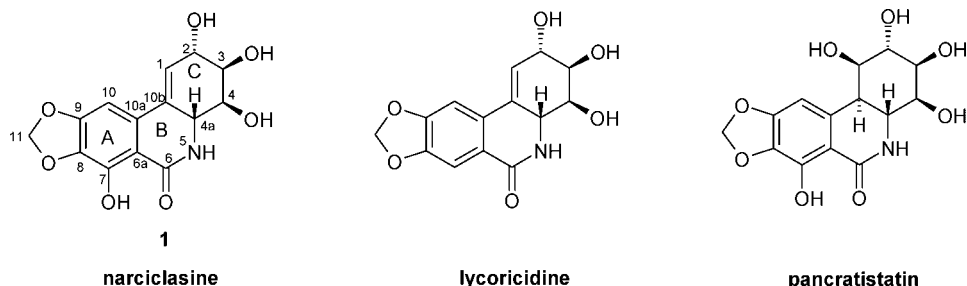


**Figure 1.** Chemical structures of narciclasine, lycoricidine, and pancratistatin.

The aim of the present study was to confirm the anticancer effects of narciclasine in apoptosis-resistant as well as in apoptosis-sensitive cancer cells and to determine whether the compound's activity results from pro-apoptotic effects or from impairment of the organization of the actin cytoskeleton of cancer cells, a process which would have a marked impact on cancer cell proliferation (cytokinesis) and migration.<sup>21,22</sup> In addition, given the total synthesis of narciclasine is still very complex and requires too many steps to be developed commercially,<sup>15,16</sup> the current study reports on the synthesis of novel analogues derived from narciclasine itself, which may be amenable to large-scale preparation.<sup>16,23,24</sup> A series of 26 novel analogues<sup>25</sup> was obtained with the further aim of determining their activity in various *in vitro* and where appropriate *in vivo* tumor models and to further establish the structure–activity-relationship (SAR) within the series and the underlying mechanism of action of narciclasine and its analogues.

**Chemistry.** For the extraction and purification of narciclasine (**1**; Figure 1), several processes can be used<sup>16,26</sup> depending on the plant species. Described here is the outline procedure used for the *Narcissus* “Carlton”. More details are provided in the Experimental Section. An ethanolic extract of fresh bulbs of the *Narcissus* “Carlton” (Ernest Turc, Angers, France) was evaporated to leave an aqueous residue, which was itself extracted with dichloromethane to remove nonpolar contaminants. Narciclasine (**1**) was then extracted from the residual aqueous phase with ethyl acetate. After evaporation of the solvent, the residue was further purified by column chromatography (see Experimental Section). Narciclasine (**1**) was obtained as the pure product after methanol crystallization of the eluted fraction containing the compound. The spectral properties (1D NMR, 2D NMR and mass spectra) of the isolated product were identical to those previously published<sup>26</sup> and confirmed the identity of the product as narciclasine (**1**). Using this procedure, 110 mg of narciclasine (**1**) was obtained from 1 kg of bulbs, which is of the same order as previously reported.<sup>15,16</sup>

To perform SAR analysis of novel narciclasine related products, all reactive positions of narciclasine (R1 with or without the double bond (dotted line in the right-hand structure of Figure 2), R2, R3, R4, R5, and X) have been modified by hemisynthesis (Figure 2). These chemical modifications, which are summarized in Table 1, involved a limited number of chemical steps, which are described in detail in the Experimental Section or the Supporting Information.

To obtain esters in position R1 and R5 (Scheme 1), we first synthesized the well-known acetonide intermediate (**2**) starting from narciclasine.<sup>27</sup> This product (**2**) was then acylated to give esters (**3a–3e**) as intermediates. The acetonide function of these compounds was then deprotected by acidic conditions to provide esters (**6a–7e**). To transform the diester (**6a**) into the monoester (**7a**), a selective hydrolysis of the phenol ester (reaction (e), Scheme 1) was used as previously published.<sup>28</sup> To obtain

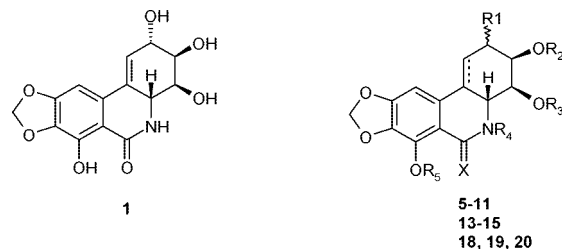


**Figure 2.** General structure of hemisynthesized derivatives of narciclasine (**1**).

modified products in position R4 and R5, we first synthesized the triacetate ester of narciclasine (**4**) as described in the literature<sup>28</sup> (Scheme 1). Compound (**4**) was then alkylated or coupled with various reagents to provide derivatives (**5f–5o**). After alkaline hydrolysis of ester functions, we obtained derivatives (**7g–8n**). Starting from product (**7o**), deprotection of one benzyl group by sodium iodide furnished the compound (**8o**).

To reduce the carbonyl lactam function of narciclasine, we also started the synthesis from the acetonide derivative of narciclasine (**2**). The alcohol function in position 2 of this compound was then protected by the silyl ether (TBDMS) to obtain product **9** (Scheme 2). The reduction by  $\text{LiAlH}_4$  followed by the deprotection of the silyl ether gave the compound (**10**). Finally, the acetonide function of this compound was then deprotected by acidic conditions to provide derivative (**11**) in which the carbonyl function of narciclasine had been reduced (Scheme 2).

To verify the influence of the carbonyl function on the cytotoxicity of this class of compound, we modified the amino group of product (**11**). To achieve this, we first synthesized urea or amide derivatives starting from compound **9** (Scheme 3). After reduction of the carbonyl and reaction with trichloroacetyl isocyanate, this intermediate gave derivative (**12**). After deprotection and hydrolysis, this furnished the urea (**13**). After the same reduction of the carbonyl followed by reaction with acetyl chloride, the intermediate gave compound (**14**). The acetonide function of this latter product was then deprotected to provide the amide (**15**) (Scheme 3).

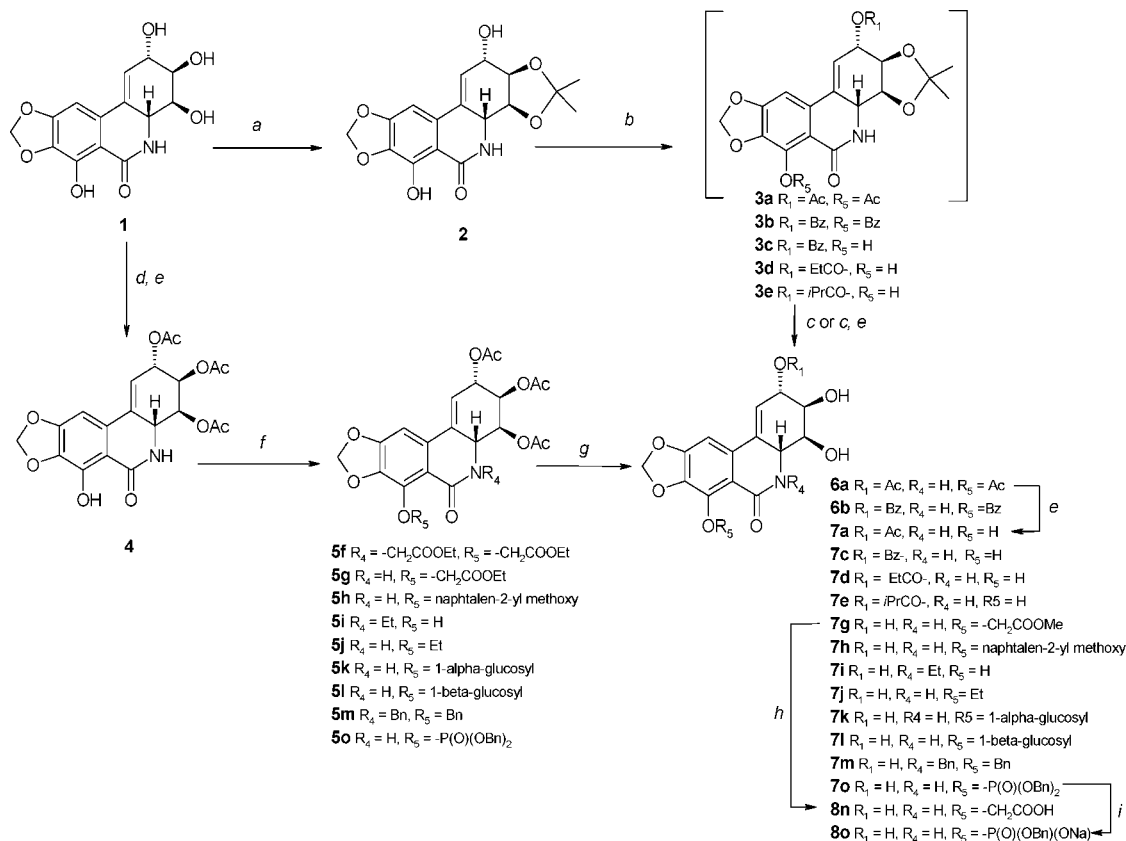
To obtain derivatives (**18**) and (**19**), catalytic hydrogenation in the presence of triethylammonium formate was performed to provide after acetonide protection compounds (**16: cis**) and (**17: trans**; Scheme 4). It is interesting to note this hydrogenation gave around 50% of the *trans*-derivative and 50% of the *cis*-derivative. These hydrogenation conditions are the best developed to date to obtain the *trans*-derivative starting from narciclasine. Swern oxidation followed by reductive amination with propylamine and deprotection of the acetonide function provided final products (**18**) and (**19**) starting from compounds (**16**) and (**17**; Scheme 4).



Table 1. Continued

	Reaction site <sup>a</sup>						IC <sub>50</sub> (μM) <sup>b</sup>							% Stability of Product <sup>c</sup>
	R1	R2	R3	R4	X	R5	PC-3	U373	BxPC3	LoVo	A549	MCF-7	Median	
<b>15</b>	.....OH	-H	-H		-CH <sub>2</sub>	-H	>10	>10	>10	>10	>10	>10	>10	96
<b>18</b>		-H	-H	-H	O	-H	>10	>10	>10	>10	>10	>10	>10	99
<b>19</b>		-H	-H	-H	O	-H	>10	>10	>10	>10	>10	>10	>10	99
<b>20</b>	.....OH	-H	-SO <sub>3</sub> Na	-H	O	-H	>10	>10	>10	>10	>10	>10	>10	100

<sup>a</sup> Chemical modification to each of **1**'s reaction sites. For these derivatives, the dotted line in Figure 2 represents a double bond. <sup>b</sup> The in vitro antiproliferative activities of the compounds are reported as IC<sub>50</sub> values (nM) determined using the MTT colorimetric assay. IC<sub>50</sub> values refer to the concentration needed to decrease the overall growth of cell lines by 50% over three days on culturing in the presence of the drug. This was carried out on six different human cancer cell lines including PC-3 prostate, U373 GBM, BxPC3 pancreas, LoVo colon, A549 NSCLC, and MCF-7 breast. <sup>c</sup> The stability of products was measured by HPLC analysis following incubation in a physiological solution at 37 °C over 7 days. Results are expressed as the % of the incubated compound recovered. <sup>d</sup> nd: not determined.

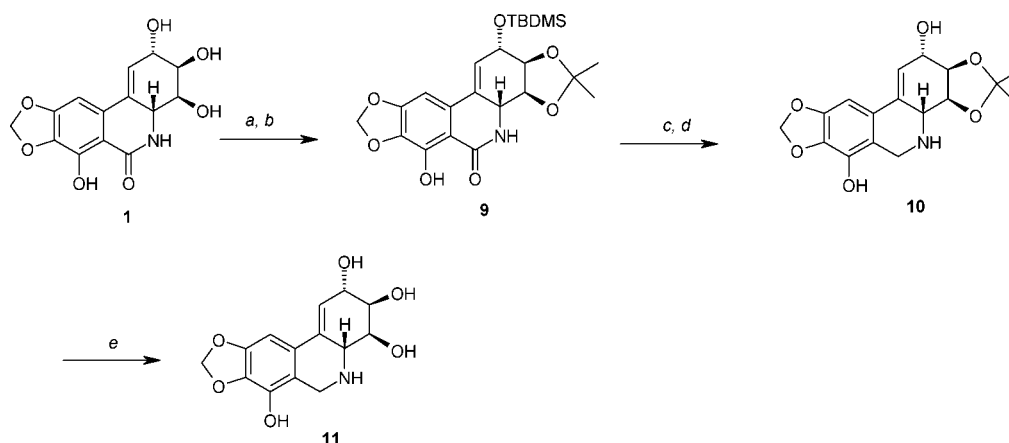
Scheme 1<sup>a</sup>

<sup>a</sup> (a) 2,2-Dimethoxypropane, PTSA, DMF. (b) Acyl anhydride or acyl chloride, pyridine or DMF. (c) TFA, H<sub>2</sub>O, THF. (d) Acetic anhydride, DMAP, pyridine. (e) H<sub>2</sub>O, pyridine, 110 °C. (f) Alkyl halide, K<sub>2</sub>CO<sub>3</sub>, DMF, or acetonitrile for (**5k**) and **5l**: 1-( $\alpha$ )-bromoperbenzoylglucose, AgOTf, allylsilane, 4 Å molecular sieves, CH<sub>2</sub>Cl<sub>2</sub>/toluene; for **5o**: dibenzyl phosphite, CCl<sub>4</sub>, DIPEA, DMAP, acetonitrile. (g) K<sub>2</sub>CO<sub>3</sub>, H<sub>2</sub>O, MeOH. (h) LiOH, H<sub>2</sub>O, dioxane, 0 °C. (i) NaI, acetone.

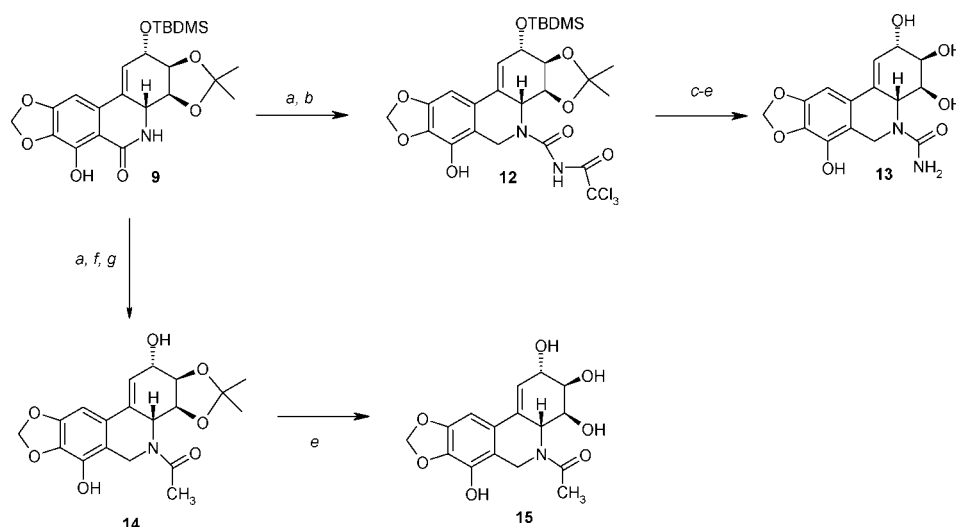
For most compounds, aqueous stability was determined at physiological pH and 37 °C (Table 1). Some compounds to be orally administered were also tested at pH 2.

**Pharmacology. Characterization of the Pro-Apoptotic Effects Induced by Narciclasine (1) in Human Cancer Cells.** As stated previously, we recently demonstrated that the in vitro growth inhibitory (antiproliferative) activity of high

narciclasine (**1**) concentrations ( $\geq 1 \mu\text{M}$ ) in carcinoma cells (cancer cells of epithelial origin) relates to pro-apoptotic effects resulting from compound-mediated triggering of the activation of the initiator caspases of the death receptor pathway.<sup>20</sup> However, Table 1 shows that the in vitro IC<sub>50</sub> growth inhibitory activity of narciclasine (**1**) in human cancer cells was well below 1  $\mu\text{M}$  and in fact in the range 30–90 nM. Narciclasine (**1**)

Scheme 2<sup>a</sup>

<sup>a</sup> (a) 2,2-Dimethoxypropane, PTSA, DMF. (b) TBDMSCl, imidazole, DMF. (c) LiAlH<sub>4</sub>, THF. (d) TBAF, THF. (e) H<sub>2</sub>SO<sub>4</sub>, H<sub>2</sub>O, THF/CH<sub>2</sub>Cl<sub>2</sub>.

Scheme 3<sup>a</sup>

<sup>a</sup> (a) LiAlH<sub>4</sub>, THF. (b) Trichloroacetyl isocyanate, MEK, 0 °C. (c) TBAF, THF. (d) K<sub>2</sub>CO<sub>3</sub>, H<sub>2</sub>O, MeOH. (e) TFA, H<sub>2</sub>O, THF. (f) Acetyl chloride, TEA, CH<sub>2</sub>Cl<sub>2</sub>. (g) TBAF, THF.

displayed similar *in vitro* growth inhibitory activity in carcinoma cells highly sensitive to pro-apoptotic insult such as human MCF-7 breast<sup>20</sup> and PC-3 prostate cancer cells<sup>20</sup> and apoptosis-resistant human U373 glioblastoma (GBM) cells.<sup>29</sup>

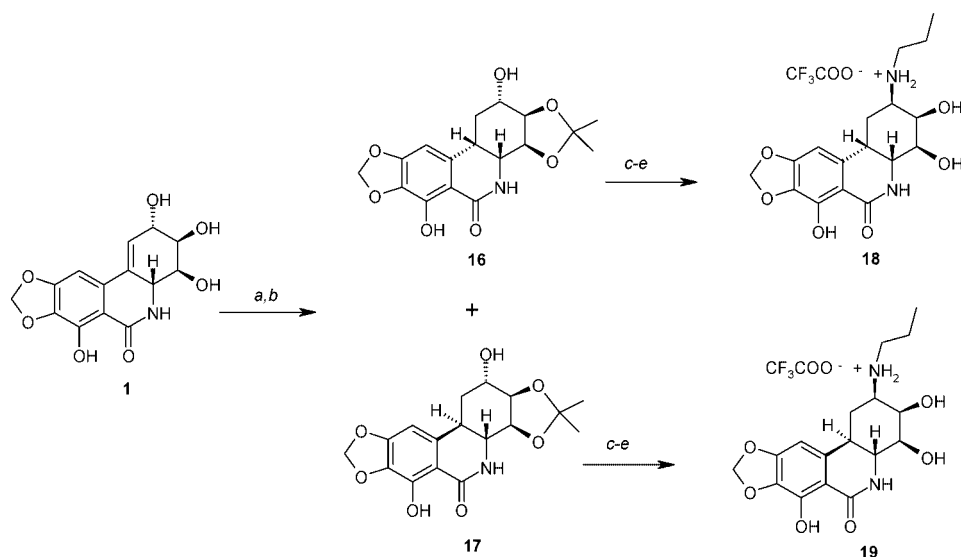
Figure 3A shows that human Hs683 GBM cells that are 1p19q deleted<sup>29</sup> (oligodendroglial in origin<sup>30</sup>) and sensitive *in vivo* to pro-apoptotic drugs<sup>29</sup> can be challenged at the level of p53 activation by a pro-apoptotic insult induced by adriamycin (ADR; used as a positive pro-apoptotic control) but not by temozolomide (TMZ; a pro-autophagic drug<sup>7</sup> used here as a negative pro-apoptotic control). TMZ can induce late apoptosis events in cancer cells but only after they have been treated for at least 5 days with TMZ.<sup>31</sup> The sensitivity of Hs683 GBM cells to the pro-apoptotic insult of adriamycin is similar to that observed in MCF-7 cells (Figure 3A), which are also sensitive to pro-apoptotic drugs.<sup>20</sup> In sharp contrast, p53 is mutated and constitutively activated (Figure 3A) in human U373 GBM cells (astroglial in origin,<sup>30</sup> not deleted with respect to 1p and 19q<sup>29</sup> and not sensitive *in vivo* to pro-apoptotic drugs<sup>29</sup>), a feature that suggests that these cells should be apoptosis-resistant.

Mitochondrial outer membrane permeabilization (MOMP) is a crucial step in the apoptotic process and is often concomitant with a decrease in mitochondrial membrane potential ( $\Delta\Psi_m$ ) as a direct consequence of the loss of integrity in the outer

mitochondrial membrane (OMM).<sup>20</sup> MOMP is lethal because it leads to the release of diverse apoptotic effectors contained in the mitochondrial transmembrane space and compromises mitochondrial energy metabolism.<sup>20</sup> Accordingly, use was made of the JC-1 dye to measure  $\Delta\Psi_m$  in untreated and narciclasine-treated U373 and MCF-7 cancer cells (positive control<sup>20</sup>). Figure 3B shows that narciclasine induced a concentration-dependent decrease in  $\Delta\Psi_m$  in MCF-7 cells but not in U373 cells. In addition, narciclasine (**1**) provoked marked pro-apoptotic and pro-necrotic processes in MCF-7 (Figure 3Ca) but not in U373 cells (Figure 3Cb).

Furthermore, the IC<sub>50</sub> growth inhibitory value of narciclasine (**1**) in the human A549 NSCLC cell line, which is also resistant to various pro-apoptotic insults,<sup>32–34</sup> was similar to those observed in apoptosis-sensitive MCF-7 and PC-3 cancer cells (Table 1). Taken together, these data strongly suggest that narciclasine (**1**) (i) exerts its antitumor effects through nonapoptotic mechanisms when evaluated *in vitro* at its IC<sub>50</sub> growth inhibitory values and (ii) displays similar IC<sub>50</sub> growth inhibitory values in apoptosis-sensitive and apoptosis-resistant cancer cells.

**Narciclasine (1) Impairs Cancer Cell Proliferation and Migration, and to a Lesser Extent Fibroblast Cell Proliferation and Migration.** The *in vitro* scratch wound assay in conjunction with computer-assisted phase-contrast microscopy

Scheme 4<sup>a</sup>

<sup>a</sup> (a) Triethylammonium formate, Pd/C, CH<sub>2</sub>Cl<sub>2</sub>/EtOH. (b) 2,2-Dimethoxypropane, PTSA, DMF. (c) DMSO, oxalyl chloride, Et<sub>3</sub>N, CH<sub>2</sub>Cl<sub>2</sub>, -78°C. (d) Propylamine, NaBH(OAc)<sub>3</sub>, DCE. (e) TFA, H<sub>2</sub>O, THF.

enabled the quantitative determination of both cell proliferation and migration.<sup>22</sup> Human U373 GBM and PC-3 prostate cancer cells and normal Ccd-25-Lu fibroblasts were grown in vitro to confluence and scratch wounds made by creating a linear denuded region using a pipet tip as illustrated at the top of Figure 4 (CT 0 h). The three cell lines studied reached confluence after 72 h. One image was taken every four minutes for each experimental treatment of the three cell lines (control, 10 and 100 nM incubation with narciclasine). The percentages of wound area recolonized were calculated every 12 h for 72 h as indicated in Figure 4. The lower narciclasine concentration did not retard wound healing. At 100 nM, narciclasine (1) displayed greater inhibitory effects in U373 compared to PC-3 cancer cells despite IC<sub>50</sub> growth inhibitory values in these two cell lines being 0.03 μM (Table 1). Thus, narciclasine (1) appears to exert its antitumor effects independent of apoptosis status: resistant (U373<sup>29</sup>) versus sensitive (PC-3<sup>20</sup>) cells. We had observed previously that normal human fibroblasts appear ~250 fold less sensitive to the antiproliferative/migratory effects of narciclasine. The compound also does not induce apoptosis in these cells probably due to the absence of death receptor pathway activation.<sup>20</sup> However, the data in Figure 4 reveal that 100nM narciclasine transiently impaired the wound healing process of normal human Ccd-25-Lu fibroblasts.

**Narciclasine (1) Impairs Actin Cytoskeleton Organization in Cancer Cells.** A common feature that can impair both cell proliferation and migration (as revealed in dynamic scratch wound assays on U373 GBM cells (Figure 4) when no cell death is evidenced (Figure 3Cb)) relates to disorganization of the actin cytoskeleton.<sup>1,22</sup> At 100 nM, narciclasine markedly increased the proportion of fibrillary polymerized actin (green fluorescence) constituting the actin cytoskeleton in both PC-3 prostate cancer (Figure 5A) and U373 GBM (Figure 5B) cells but not in Ccd-25-Lu normal fibroblasts (Figure 5C). Quantitative determination using computer-assisted fluorescence microscopy (Figure 5D) revealed that 100 nM narciclasine indeed markedly increased the levels of fibrillary actin in PC-3 and U373 cancer cells ( $p < 0.001$ ) but not in Ccd-25-Lu normal cells ( $p > 0.05$ ). This increase renders the actin cytoskeleton in cancer cells more rigid, a process that can lead to the impairment of growth (Table 1) and migration (Figure 4).

**Structure–Activity Relationship Analyses.** Table 1 reveals that almost none of the chemical modifications to narciclasine (1) improved its antiproliferative IC<sub>50</sub> values as revealed by the MTT colorimetric assay. Only esters of the hydroxyl at position R1 (7c–7e) apparently maintained/possibly improved the in vitro antitumor activity of narciclasine (Table 1), while ester (7a) had a ~10 fold weaker activity. This type of modulation of lycoricidine (Figure 1) had previously been reported to give similar results.<sup>15,16,35</sup> This may not be surprising given that certain derivatives with ester function at R1 were revealed to be appreciably unstable in aqueous media at 37 °C (Table 1). The decomposition of these products determined by HPLC analysis (Table 1) gave narciclasine and, more surprising, narciprimine (for the chemical structure, see ref 16). Therefore, the antiproliferative activity observed with these ester derivatives may merely reflect in part the activity of the released parent, narciclasine. Narciprimine was obtained by elimination of the ester group in the allylic position (good leaving group) and subsequent aromatization of ring C. Diesters on positions R1 and R5 (6a and 6b, Table 1) resulted in growth inhibitory activity on cancer cells similar or weaker than corresponding monoester derivatives (7a, 7c). These latter data suggested that a free phenolic hydroxyl group at position R5 provides optimal antitumor activity.<sup>15,16</sup> Given the ready instability of monoesters (elimination of the ester group), further synthetic effort was directed to obtaining more stable products, notably amino derivatives at position R1 (weaker leaving group). To provide this kind of compound with a propylamino function, the double bond (dotted line, Figure 2) had to be removed because all activated intermediates with double bonds were unstable. Two amino compounds (18 and 19) were stable in aqueous media at 37 °C but failed to demonstrate significant antitumor activity in vitro (Table 1). This result was perhaps not surprising for the *cis*-derivative (18) because it is known that the *trans*-B/C ring junction (without the double bond between C-10a and C1) is essential to maintain potent cytotoxicity for this type of compound.<sup>15,16</sup> In contrast, the absence of antitumor activity for the *trans*-derivative (19) was more surprising given this product does not have the double bond but has the required *trans*-B/C ring junction to maintain cytotoxic activity. As position R1 tolerates steric hindrance (given that product (7c)

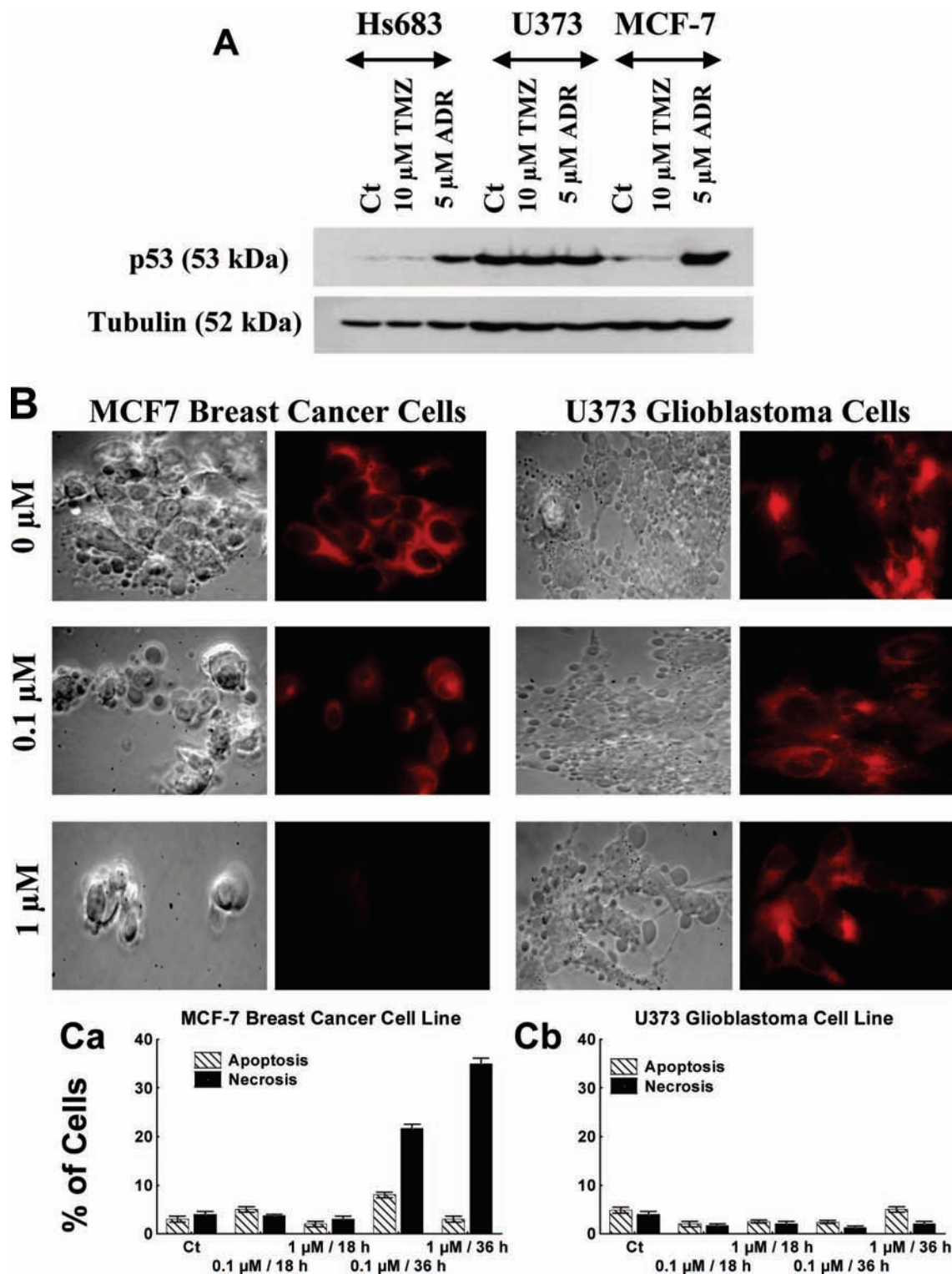


**Figure 3.** (A) Western blotting analyses of p53 expression after having cultured Hs683 (oligodendroglioma), U373 (astroglioma), and MCF-7 (breast) cancer cells for 24 h in the presence of 10  $\mu$ M temozolomide (TMZ: a pro-autophagic drug) and 5  $\mu$ M adriamycin (ADR: a pro-apoptotic drug). (B) Involvement of mitochondria in apoptotic cell death induced by narciclasine: JC-1 staining of MCF-7 and U373 cells either untreated ("0  $\mu$ M") or compound treated with 0.1 or 1  $\mu$ M for 24 h. Red fluorescence resulting from JC-1 staining is specific to mitochondria with an intact mitochondrial membrane potential of  $\Delta\Psi_m$ . Mitochondrial outer membrane permeabilization, which is a direct consequence of the loss of integrity in the outer mitochondrial membrane, is a crucial step in the apoptotic process and is visualized through the loss of JC-1 staining in MCF-7 cancer cells only.

with a benzoyl group reveals potent cytotoxicity), compound (19)'s lack of antitumor activity could not be attributed to the steric hindrance of the propylamino group. It could however, result from inappropriate stereochemistry at position 2 during

its hemisynthesis: *R*-configuration for (19) in contrast to the *S*-configuration for narciclasine (1). The *C*-2 configuration seems therefore to be essential for the antitumor activity of this type of compound. The hydroxyl functions at positions R2 and R3

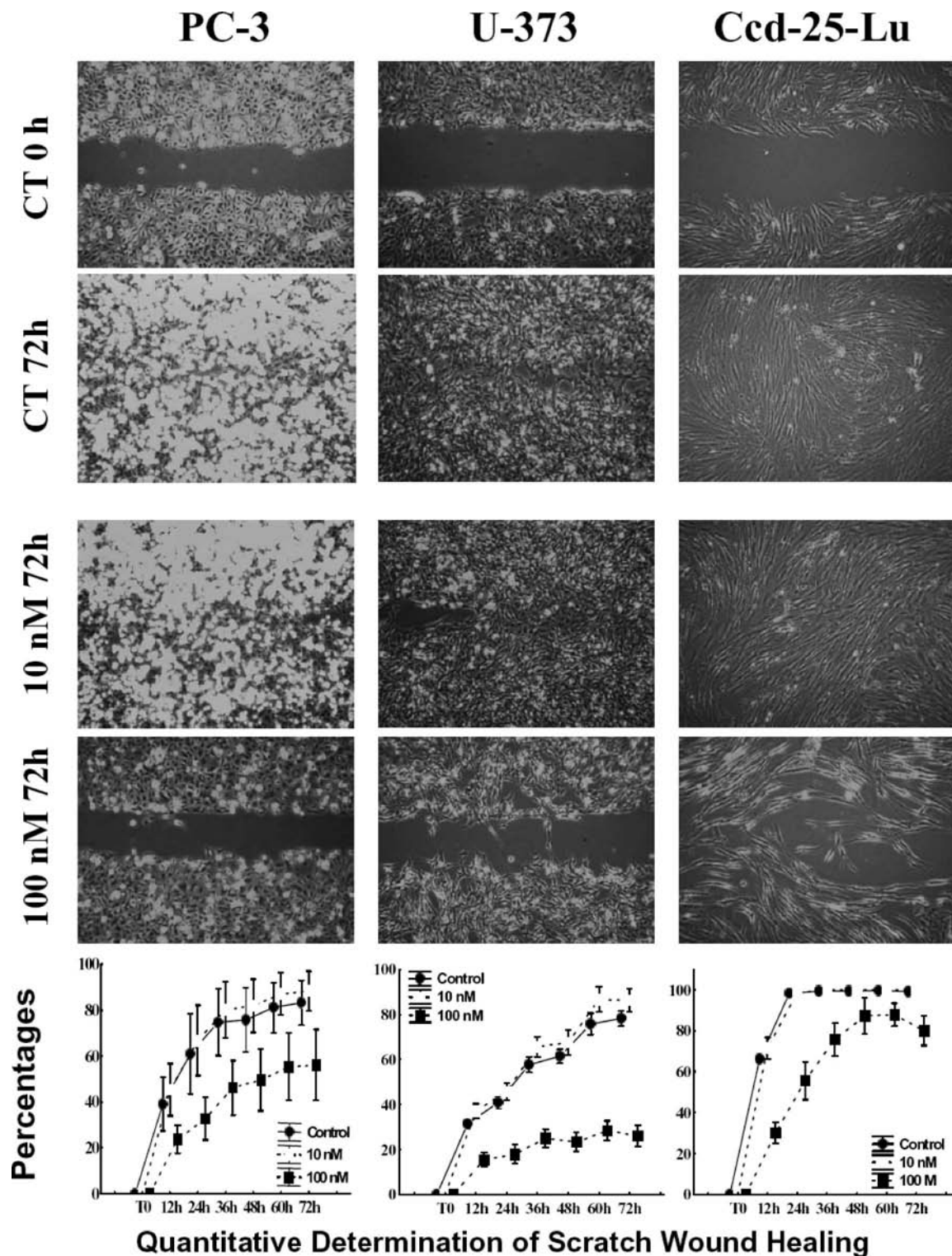


**Figure 4.** Scratch wound assays of human PC-3 prostate cancer cells, U373 glioblastoma cells, and normal Ccd-25-Lu lung fibroblasts treated for 72 h with 10 or 100 nM narciclasine. The percentage wound healing which occurred over a 72 h period of observation was quantitatively determined by means of computer-assisted videomicroscopy as detailed previously.<sup>40,47</sup>

also seem essential on analyzing the antitumor activity obtained for **9**, **10**, and **20**, as already reported in the literature.<sup>15,16,36,37</sup> All modifications made to positions R4 and X led to compounds devoid of antitumor activity in vitro (**5f**, **7i**, **7m**, **10**, **11**, **13**, and **15**). The lactam carbonyl function with no substitutions on the nitrogen atom seems therefore to be necessary for antitumor activity. The activities of compounds with modulation of position R5 were found to be at least 100 times less potent (**5h**,

**7g**, **7h**, **7k**, **8n**) than narciclasine or even inactive (**5g**, **7i**, **7j**). These data appear to confirm that the phenolic hydroxyl group at position R5 of narciclasine is mandatory for antitumor activity.<sup>15,16</sup>

**Narciclasine (1) Displays Higher In Vitro Antiproliferative Effects in Cancer than Normal Cells.** The growth inhibitory effects of narciclasine (**1**) on 19 human and 3 rodent cancer cell lines, and 6 normal cell lines including 3 fibroblast



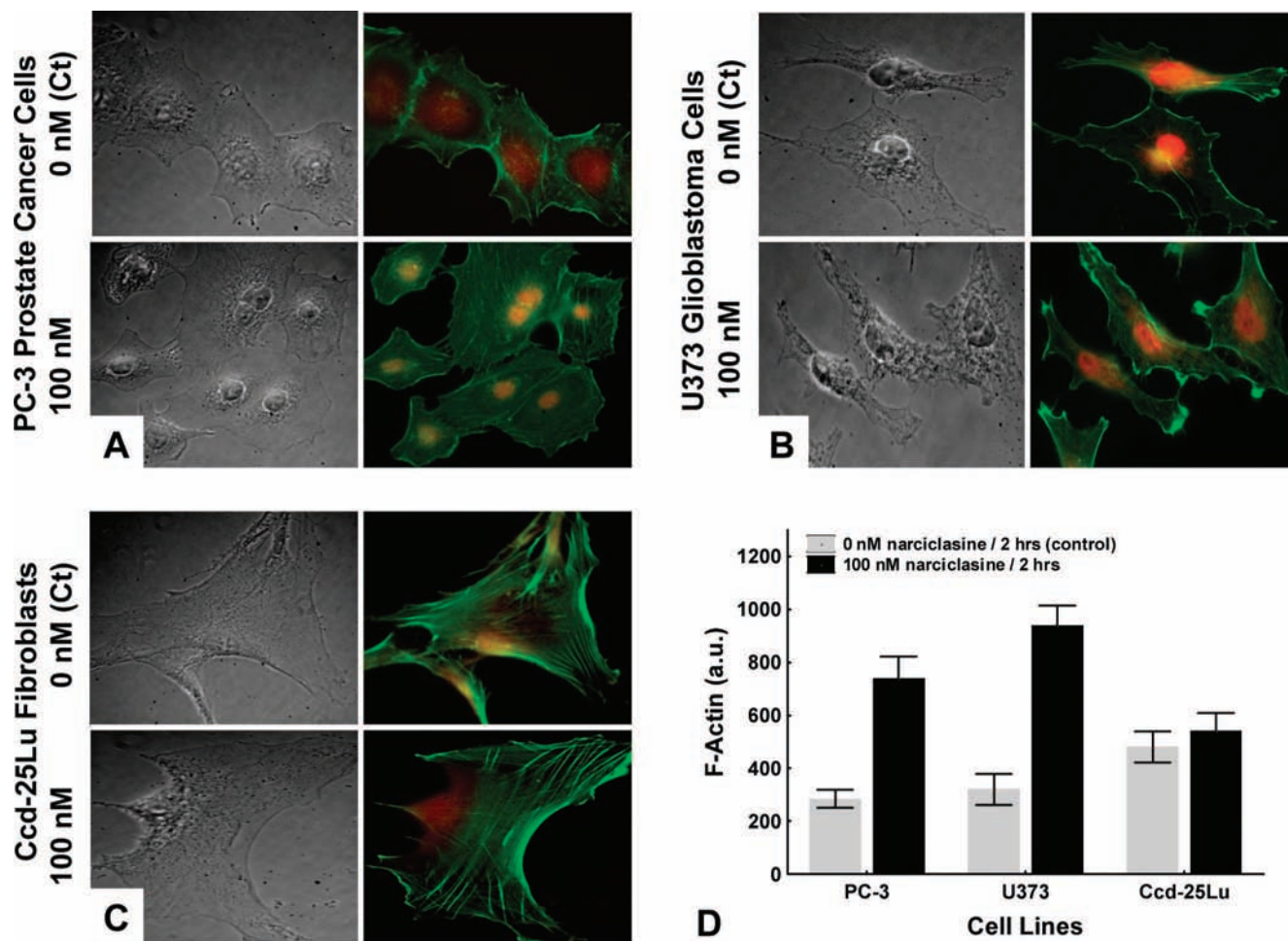


**Figure 5.** Qualitative (A–C) and quantitative (D) determination of narciclasine-induced effects on actin cytoskeleton organization in human PC-3 prostate cancer cells (A), U373 glioblastoma cells (B), and normal Ccd-25-Lu lung fibroblasts (C). Fibrillar actin and globular actin appear as green and red fluorescence, respectively. The levels of fibrillar actin was quantitatively determined by means of computer-assisted fluorescence microscopy as detailed previously.<sup>47</sup>

and 3 human umbilical vein endothelial cell (HUVEC) lines were determined (Table 2). The data show that narciclasine (**1**) displayed potent antiproliferative activity independent of the tumor type and independent of whether the cells were of human ( $IC_{50}$  range 5–99 nM) or rodent origin ( $IC_{50}$  range 28–35 nM). Narciclasine (**1**) exerted markedly weaker effects on normal fibroblasts than on tumor cells ( $IC_{50}$  values  $\geq$  317 nM). The compound's antiproliferative effect on HUVEC cells was closer to that observed in tumor cells ( $IC_{50}$  range 87–94 nM). These data thus suggest that in addition to displaying potent antitumor effects, narciclasine (**1**) could also display antiangiogenic effects. The fact that the compound displays antiproliferative and antimigratory (data not shown) effects on tumor cells and HUVECs, could relate at least partly to the fact that actin, a clear target for narciclasine (Figure 5), is key to migration and proliferation processes in both tumor cells and endothelial cells.<sup>21,22</sup>

**Pharmacokinetics of Narciclasine (**1**) and its Prodrug (**7k**) in Vivo in Healthy Mice.** As indicated above, most hemisynthesized derivatives of narciclasine in the current study resulted in products with generally lower inhibitory effects than narciclasine on both the proliferation and migration of cancer cells. Accordingly, it was considered appropriate to evaluate potential prodrugs of narciclasine with respect to their ability to demonstrate notably improved oral bioavailability and activity in vivo. Indeed the mechanisms involved in prodrug cleavage

which are well documented in vivo, are believed to operate in the case of narciclasine 4-*O*- $\beta$ -D-glucopyranoside, which has shown comparable anticancer activity to narciclasine.<sup>38</sup> Although similar mechanisms that convert **7k** into narciclasine could operate for the esters **4**, **6a**, **7a–7e**, and the glycosyl derivatives **5k** and **5l**, among the prodrugs synthesized, compound **7k** which displays 92% stability at physiological pH 7.4 (Table 1) and is <20% degraded in 1 h at pH 2 (Figure 6C) was considered to be a suitable candidate (Figure 6) for further evaluation. High chemical stability at pH 7.4 and pH 2 were considered important to the potential pharmaceutical development of respectively iv and oral formulations of these narciclasine prodrugs.

Figure 6A illustrates narciclasine (**1**) plasma concentrations after either single administration of the compound at 10 mg/kg po (open circles) or 5 mg/kg iv (crosses) or repeat administration at 5 mg/kg iv for 5 days (5x1w) to female B6D2F1 (Charles River) mice. Post oral dose, narciclasine (**1**) revealed peak plasma concentrations of  $\sim$ 300 ng/mL, and an overall systemic exposure reflected in an  $AUC_{0-24\text{ h}}$  of 50129 ng $\cdot$ min/mL. When compared to the post iv  $AUC_{0-24\text{ h}}$  of 81132 ng $\cdot$ min/mL, this confirmed the oral bioavailability of narciclasine (**1**) in mice to be 32%. Post iv, narciclasine was cleared rapidly, with a terminal elimination half-life of 66 min. Furthermore, comparison post iv of terminal elimination half-life values after single (1x1w; 66 min) versus repeat (5x1w; 58 min) administration indicated no marked change (day 1 versus day 5), suggesting that

**Table 2.** Determination of Antiproliferative IC<sub>50</sub> Values for Narciclasine in 6 Normal and 22 Cancer Cell Lines<sup>a</sup>

human carcinoma			human normal			rodent carcinoma		
histological group	cell lines	IC <sub>50</sub> (nM)	histological group	cell lines	IC <sub>50</sub> (nM)	histological group	cell lines	IC <sub>50</sub> (nM)
<b>central nervous system</b>	U373	29	<b>lung fibroblast</b>	WI-38	317	<b>CNS</b>	C6	28
	U-87	98		Ccd-25-Lu<	>10000		9 L	32
	T98G	48	<b>skin fibroblast</b>	WS-1	>10000	<b>melanoma</b>	B16F10	35
	Hs683	40		<b>vein endothelial cells</b>	HUVEC (HTG04)		87	
	Daoy	22	HUVEC (HTG06)		97			
FaDu	8	HUVEC (HTG07)	94					
<b>head and neck</b>	RPMI 2650	14						
	Detroit 562	6						
	<b>melanoma</b>	SKMEL-28	37					
		HT144	38					
<b>prostate</b>	G361	99						
	C32	25						
	PC-3	28						
<b>pancreas</b>	BxPC-3	28						
	<b>colorectal</b>	LoVo	94					
		HCT-15	32					
<b>lung</b>	A549	29						
	<b>breast</b>	MCF-7	45					
		Mda-Mb-231	5					
	<b>mean ± SEM</b>	38 ± 6			<i>b</i>		32 ± 2	
	<b>median</b>	31			207		32	
	<b>IC<sub>50</sub> min</b>	5			94		28	
	<b>IC<sub>50</sub> max</b>	99			>10000		35	

<sup>a</sup> U373 (ECACC code 89081403), U-87 (ECACC code 89081402), T98G (ATCC code CRL-1690), G361 (ATCC code CRL-1424), C32 (ECACC code 87090201), and C6 (ATCC code CCL-107) cell lines were cultured in MEM medium supplemented with 5% heat inactivated fetal bovine serum. Hs683 (ATCC code HTB-138), FaDu (ATCC code HTB-43), RPMI 2650 (ATCC code CCL-30), Detroit 562 (ATCC code 138), SKMEL-28 (ATCC code HTB-72), PC-3 (DSMZ code ACC465), BxPC-3 (ECACC code 93120816), LoVo (DSMZ code ACC350), HCT-15 (DSMZ code ACC357), A549 (DSMZ code ACC107), MCF-7 (DSMZ code ACC115), 9L (ATCC code CRL-2200), and B16F10 (ATCC code CRL-6475) cell lines were cultured in RPMI medium supplemented with 10% heat inactivated fetal bovine serum. HT-144 (ATCC code HTB-63), WI-38 (ATCC code CCL-75), and Ccd-25-Lu (ATCC code CCL-215) were cultured in MEM medium supplemented with 10% heat inactivated fetal bovine serum and 100 μM nonessential amino acids. Daoy (ATCC code HTB-186) and WS-1 (ECACC code 88021104) were cultured in MEM medium supplemented with 10% heat inactivated fetal bovine serum. Endothelial cells obtained from the veins of human umbilical cords were cultured in EGM-2 MV Bullet Kit. MEM and RPMI cell culture media were supplemented with 4 mM glutamine, 100 μg/mL gentamicin, and penicillin–streptomycin (200 U/mL and 200 μg/mL). <sup>b</sup> The mean IC<sub>50</sub> value could not be determined as one or more of the corresponding data points were higher than the threshold value.

**Table 3.** Summary of Narciclasine Toxicity in Female Wistar Rats

assessment	narciclasine administered 5 times per week for 3 weeks at dose levels			
	25 mg/kg/day	10 mg/kg/day	3 mg/kg/day	1 mg/kg/day
general observations	8/11 rats found dead on day 3 and the remaining animals sacrificed for ethical reasons	all rats sacrificed on day 3 for ethical reasons	no deaths	no deaths
clinical observations	days 1–3: piloerection and diarrhea.	days 1–3: piloerection, diarrhea, hunched posture, and lethargy	hunched posture, piloerection from 2nd week onward with signs appearing about 1 h postdose	no clinical signs
body weight (BW)	no data available	severe BW loss (11%) on day 3	slight BW loss during week 1 and week 2	no BW loss
blood cell parameters and biochemistry	alterations in red and white blood cell parameters.	alterations in red and white blood cell parameters	increase in white blood cell count but decrease in red blood cell count and hematocrit; increase in alanine aminotransferase activity, decrease in creatinine, sodium, and chloride concentrations but increases in cholesterol, triglyceride, phospholipid, potassium, and calcium levels.	minimal increases in cholesterol, triglycerides, phospholipids, potassium, and calcium concentrations
macroscopy	stomach abnormalities, red foci on thymus, thymic atrophy, and autolysis	stomach abnormalities, but to lesser extent than at 25 mg/kg/day, emaciation, and thymic atrophy	irregular surface of the fore stomach (5/5 rats) and foci in the stomach (1/5 rats)	no findings
microscopy	glandular gastric lesions of individual cell necrosis in superficial mucosa	glandular gastric lesions of individual cell necrosis in superficial mucosa; inflammatory and degenerative cecal mucosal lesions (2/5 rats), keratinized forestomach with lesions of acanthosis (1/5 rats)	keratinized forestomach acanthosis and hyperkeratosis (5/5 rats), with mild erosion (1/5 rats)	minimal acanthosis in the keratinized forestomach mucosa (2/5 rats)

narciclasine (**1**) has no effects on CYP enzyme activity with respect to its own metabolism.

Figure 6B illustrates plasma concentrations of compound **7k** after single iv administration of 5 mg/kg of **7k** (black circles) and of compound **7k** (black triangles) and narciclasine (**1**; open

triangles) after single oral administration of 10 mg/kg of **7k** to female B6D2F1 mice. The data indicate that compound **7k** is incompletely transformed into narciclasine (**1**) when administered orally. For **7k**, its AUC<sub>0–24 h</sub> post iv was determined to be 254261 ng·min/mL and its AUC<sub>0–72 h</sub> post oral administration

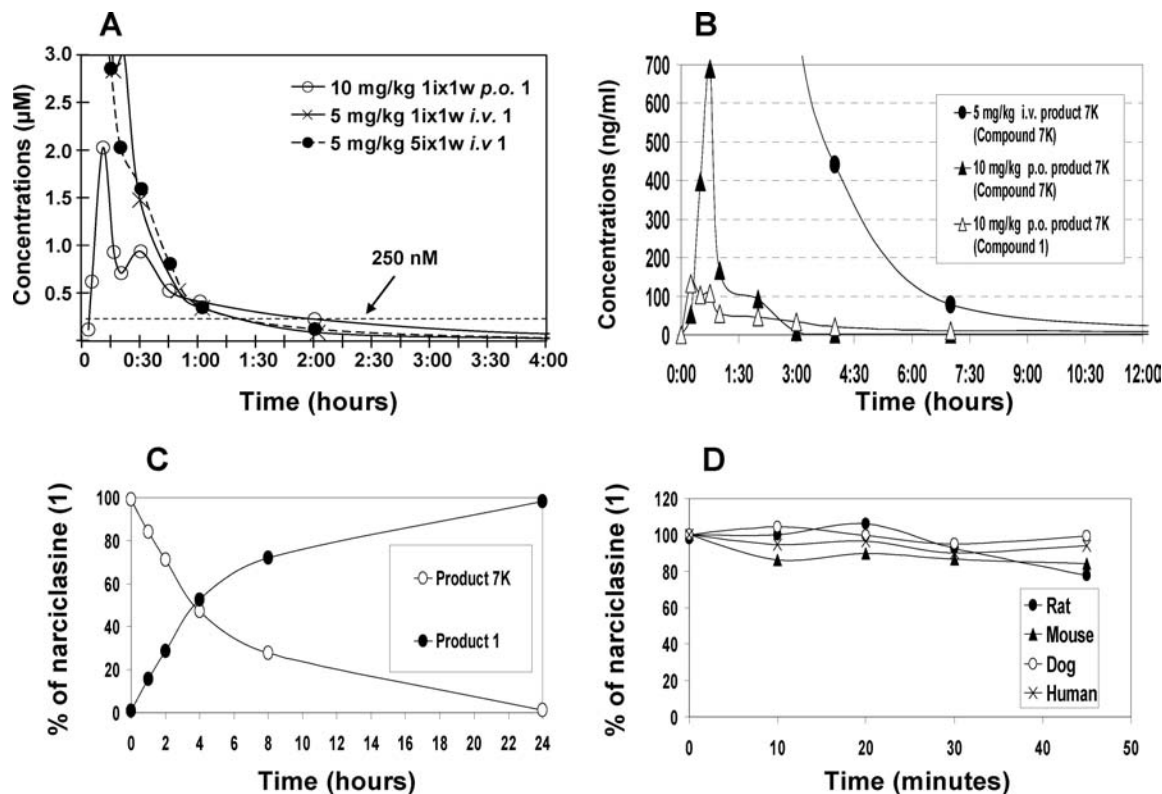


**Figure 6.** Narciclasine pharmacokinetics and in vitro metabolism and stability. (A) Mean plasma concentrations of narciclasine (**1**) after a single administration to mice ( $n = 3$ ) iv or po doses at 5 and 10 mg/kg, respectively, formulated in 5% 2-hydroxypropyl- $\beta$ -cyclodextrine. Plasma concentrations of **1** were determined using a validated LC-MS/MS method with a linear range of 2.5–1000 ng/mL (0.01 to 3.26  $\mu$ M). (B) Plasma concentrations of narciclasine (**1**) after single oral administration of compound **7k** at a dose level of 10 mg/kg (open triangles) and of compound **7k** after single iv administration of 5 mg/kg (black circles) or a single oral administration of 10 mg/kg (black triangles) of compound **7k** formulated in 5% HPBCD. (C) In vitro release of narciclasine (black circles) from compound **7k** (open circles) in aqueous media at 37 °C and pH 2. Kinetic degradation of compound **7k** was followed using an HPLC-UV method. (D) In vitro metabolic stability of narciclasine (**1**) using liver microsomes from different species. The metabolism of narciclasine (**1**) was followed using a LC-MS method.

was 29740 ng·min/mL to give an overall oral bioavailability of 5.8% for **7k**. The  $AUC_{0-72\text{ h}}$  of narciclasine (**1**) post oral administration of compound **7k** (10 mg/kg) was calculated to be 54812 ng·min/mL, which when dose normalized (for differences in molecular weight between compound **7k** and narciclasine) and compared to the narciclasine (5 mg/kg) post iv  $AUC_{0-24\text{ h}}$  of 81132 ng·min/mL gives an improved absolute bioavailability of ~52% for narciclasine (**1**) after oral administration of **7k**.

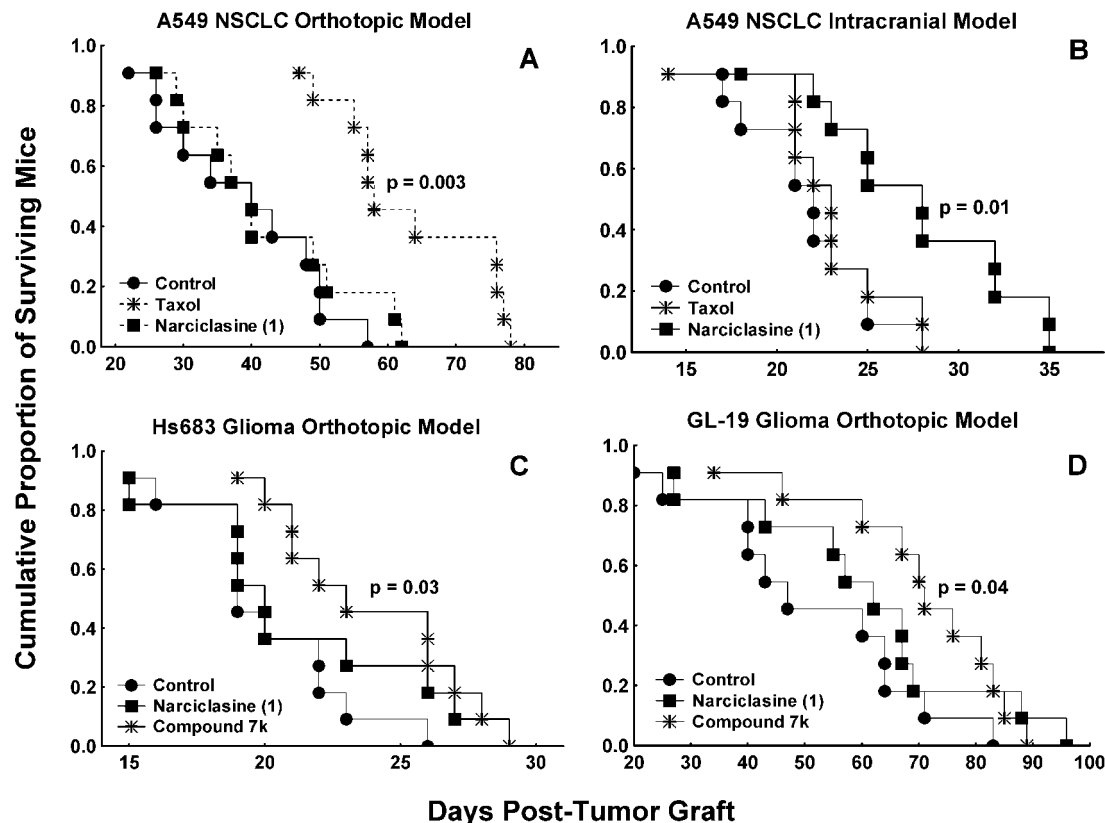
Figure 6C illustrates the in vitro release of narciclasine (**1**; black circles) from compound **7k** (open circles) in aqueous media at 37 °C and pH 2. Narciclasine (**1**) was the major product detected in the incubation and conversion was complete after 24 h under these conditions.

Figure 6D reveals that narciclasine (**1**) appears to be appreciably metabolically stable in mouse, rat, dog, and human hepatic microsomes although there appears to be a slight decline ( $\leq 20\%$ ) in rodent species after 45 min incubation. This may indicate that cytochrome P450 isozymes may not play a major role in the metabolism of the compound.

**Narciclasine (1) Toxicity in Rats.** Narciclasine (**1**) formulated in 15% (w/v) aqueous 2-hydroxypropyl- $\beta$ -cyclodextrine (HPBCD) was administered by oral gavage for 5 consecutive days (Monday–Friday) for 3 weeks to female Wistar rats at dose levels of 0 (group 1), 1 (group 2), 3 (group 3), 10 (group 4), and 25 (group 5) mg/kg/day. Each group consisted of five animals. In addition, satellite animals were allocated to each treatment group for toxicokinetic assessment of drug exposure. The following investigations were undertaken: clinical signs,

body weight, food consumption, biochemical parameters, macroscopy at termination, organ weights, and histopathology on an extensive list of tissues. The resulting data, which are summarized in Table 3, reveal significant toxicity and/or lethality at the two highest dose levels. For the regimen used, the no-effect dose level (NOEL) could not be established for narciclasine (**1**) and is  $< 1$  mg/kg/day po, while the no-adverse-effect level (NOAEL) was defined to be 1 mg/kg/day po, with the minimal acanthosis reactive changes and minor variations in some biochemistry parameters observed at this dose level considered to be nonadverse. We accordingly used this NOAEL of 1 mg/kg/day po to compare the in vivo antitumor effects of narciclasine (**1**) and of compound **7k**, as detailed below.

**Characterization of the In Vivo Anti-Tumor Activity of Narciclasine (1) and its Prodrug (7k) in Human Xenograft Models.** As already indicated earlier, the human A549 NSCLC model resists various pro-apoptotic insults<sup>32–34</sup> and we accordingly used this model to investigate the in vivo antitumor effects of narciclasine (**1**). We orthotopically grafted A549 NSCLC cells in two distinct locations, either into the lungs of immunocompromized mice as detailed previously<sup>32,39</sup> or into their brains to mimic brain metastases. Taxol was used as a reference compound. Figure 7A shows that a single iv administration of narciclasine (**1**) per week at 1 mg/kg for five consecutive weeks (1ix5w schedule), did not increase the survival of mice (black squares) compared to control animals (black circles). Taxol administered iv at 20 mg/kg according to this 1ix5w schedule (stars) significantly increased the survival of A549 NSCLC xenograft-bearing mice (Figure 7A). The reverse was observed



**Figure 7.** Activity in orthotopic models of human NSCLC and glioma in immunocompromized mice. (A–B) The impact of iv administered narciclasine (**1**) and taxol on the survival of immunocompromized mice orthotopically grafted into their lungs (A) or brains (B) with human A549 NSCLC.<sup>32</sup> Taxol was administered once per week (Monday) at 20 mg/kg for five consecutive weeks with treatment starting on the 7th day post-tumor graft, while narciclasine was administered to the same schedule but at 1 mg/kg. (C) The impact of iv administered narciclasine (**1**) and compound **7k** on the survival of immunocompromized mice orthotopically grafted into their brains with human Hs683 anaplastic oligodendroglioma cells ( $3 \times 10^4$  cells/graft).<sup>29,30,40,41</sup> The two compounds were administered five times a week (Monday–Friday) at 1 mg/kg for three consecutive weeks, with treatment starting on the 7th day post-tumor graft. (D) The impact of orally administered narciclasine (**1**) and compound **7k** on the survival of immunocompromized mice orthotopically grafted into their brains with human GL-19 glioblastoma cells ( $2 \times 10^6$  cells/graft). The two compounds were administered once a week (Monday) at 1 mg/kg for five consecutive weeks, with treatment starting on the 7th day post-tumor graft.

when A549 NSCLC cells were grafted into the brains of immunocompromized mice (Figure 7B). These data suggest that narciclasine (**1**) could readily penetrate the blood–brain barrier (Figure 1). We therefore then made use of two human glioma models to compare the antitumor effects contributed *in vivo* by narciclasine (**1**) and its prodrug **7k**. The first was the Hs683 anaplastic oligodendroglioma model<sup>29,30</sup> that grows and develops very aggressively in the brains of immunocompromized mice.<sup>40,41</sup> We accordingly used an intensive iv treatment schedule of “5ix3w” 1 mg/kg/day for narciclasine (**1**) and compound **7k**. While narciclasine (**1**) failed to significantly increase the survival of Hs683 xenograft-bearing mice, compound **7k** did (Figure 7C). The second model evaluated GL-19 was a GBM primoculture established in our facilities as detailed previously.<sup>42</sup> This model was used to compare the oral *in vivo* antitumor effects of narciclasine (**1**) and its prodrug **7k**. The data in Figure 7D show that narciclasine administered orally at 1 mg/kg/day using a 1ix5w schedule did not significantly increase the survival of GL-19 GBM orthotopic xenograft-bearing mice, while its prodrug **7k** did.

## Discussion

We have recently shown that narciclasine when used at 1  $\mu$ M *in vitro* induces marked apoptosis-mediated cytotoxic effects in human carcinoma cells but not in normal fibroblasts.<sup>20</sup> Griffin et al.<sup>43</sup> also observed selective cytotoxicity of pancratistatin

toward normal and cancer cells. Narciclasine-mediated proapoptotic effects in carcinoma cells at high concentrations result from the activation of the initiator caspases of the death receptor pathway (caspase-8 and -10), at least in human MCF-7 breast and PC-3 prostate carcinoma cells.<sup>16</sup> However, it should be emphasized that the concentration of 1  $\mu$ M used in this previous study<sup>20</sup> is  $\sim 20$  times higher than the mean antiproliferative  $IC_{50}$  value against cancer cells *in vitro*, which is around 50 nM. The data from the present study also show that even at 1  $\mu$ M narciclasine does not elicit apoptosis and/or necrosis in apoptosis-resistant U373 GBM cells (Figure 3). At 50 nM, narciclasine blocks mitosis in carcinoma and glioma (and also melanoma: data not shown) cells by a mechanism of action that is not yet fully elucidated. Quantitative videomicroscopy has revealed that in fact narciclasine markedly impairs cancer cell migration; not only of PC-3 prostate (Figure 4) and MCF-7 breast cancer (data not shown) cells but also of U373 GBM cells (Figure 4), a feature which is paralleled by loss of tumor cell polarity (data not shown). We report in the present study that narciclasine induces a rapid increase in F-actin concentration (principally at the cortical cell location) in U373 GBM and PC-3 prostate cancer cells but not in normal fibroblasts (Figure 5). This sharp increase in the concentration of F-actin can in turn rigidify the actin cytoskeleton and thus impair both cell proliferation and migration. Preliminary data from our group also reveal that the narciclasine-induced increase in F-actin is

associated with a dramatic modification in serine/threonine phosphoprotein expression levels (manuscript submitted for publication). In addition, as altered cofilin expression or activity controlled by phosphorylation are associated with actin dynamics, which in turn are associated with normal<sup>44</sup> and cancer<sup>45</sup> cell proliferation and migration, the effects of narciclasine on cofilin phosphorylation status have been investigated. We have observed that narciclasine treatment significantly and rapidly increases cofilin phosphorylation (manuscript submitted for publication). Our data are in accord with the pioneering work of Ceriotti<sup>17</sup> and Carrasco et al.,<sup>18</sup> as it has become evident over recent years that a large fraction of mRNA is tightly associated with the cytoskeleton.<sup>46</sup> Whereas microtubules (polymers of tubulin) are involved in RNA-cytoskeletal association in large cells like oocytes, neurons, or oligodendrocytes, microfilaments (polymers of actin) play the major role in smaller somatic cell types.<sup>46</sup> Association of RNA with cytoskeletal filaments is clearly required for mRNA transport but also appears to be crucial for efficient protein synthesis.<sup>46</sup>

As recently emphasized by Kornienko and Evidente,<sup>16</sup> the early activity studies conducted by Ceriotti<sup>17</sup> in 1967 revealed that sc narciclasine injections at a dose of 0.9 mg/kg to mice bearing the aggressive sarcoma 180 model resulted in complete disappearance of mitoses 4 h after administration. Thus, the impairment of mitotic processes seems to be one of the major endpoints of the compound's antitumor effects, as indicated by the pioneering investigations of Ceriotti<sup>17</sup> and our current study.

The current study has additionally confirmed the oral NOAEL in rats to be 1 mg/kg/day using a schedule of 5ix3w (Table 3). The NOAEL dose should be > 1 mg/kg/day with respect to a treatment schedule involving narciclasine administration once a week for 3–5 consecutive weeks. Toxicology evaluations are ongoing in healthy mice to define the NOAEL in this species. Narciclasine has been demonstrated to be orally available with an absolute bioavailability of 32% determined in mice.

This current study has failed to deliver novel narciclasine derivatives displaying higher antiproliferative activity *in vitro* than narciclasine itself (Table 1). In this study, narciclasine administered *iv* at 1 mg/kg using a "1ix5w" schedule, failed to increase the survival of mice bearing orthotopic lung grafts of A549 NSCLC. However, the compound was significantly active using the same dose and schedule if A549 NSCLC cells were grafted into the brain of mice (mimicking brain metastases), a model in which taxol, which does not appreciably cross the blood–brain barrier, failed to demonstrate any activity. This latter result may indicate the ready penetration of narciclasine into the brain. Studies to confirm this are ongoing.

Given the failure to obtain novel derivatives with increased potency, a prodrug strategy was also investigated in an attempt to enhance the *in vivo* activity of narciclasine itself. The antitumor effects *in vivo* of narciclasine (**1**) and its prodrug **7k** were determined in two human GBM models (Hs683 and GL-19) at a dose level of 1 mg/kg/day and a treatment schedule of "5ix3w" either *iv* or oral. While narciclasine (**1**) failed to significantly increase the survival of GBM xenograft-bearing mice in either model at this dose and schedule, compound **7k** significantly increased survival times in both models. The prodrug strategy would appear to have improved the *in vivo* antitumor activity of narciclasine.

Post oral dose, prodrug **7k** was found to increase the absolute bioavailability of narciclasine to ~52%.

In conclusion, narciclasine, a plant growth regulator whose antitumor effects have been evidenced in traditional medicine going back millennia, could represent a novel weapon against

many types of cancers, including apoptosis-resistant cancers associated with dismal prognoses, as the compound impairs actin cytoskeleton organization. The actin cytoskeleton is implicated in both cell proliferation and cell migration (including the metastatic process). Narciclasine is significantly more toxic to cancer than normal cells. The current study reveals that chemical modification to the narciclasine backbone led to a certain instability among synthesized esters and even among stable derivatives only led to weakly active molecules or even to complete loss of antitumor activity *in vitro*. In contrast, one narciclasine prodrug (compound **7k**) demonstrated higher *in vivo* antitumor activity than narciclasine itself.

## Experimental Section

**Chemistry. Extraction and Isolation of narciclasine (1).** Fresh bulbs of the narcissus "Carlton" (500 g) were homogenized and ethanol (1 L) added. The mixture was stirred mechanically at room temperature for 24 h. After filtration, the residue was resuspended in ethanol (1 L) for 2 h and then refiltered. The filtrates from these two steps were then combined and concentrated under reduced pressure until the ethanol was essentially removed (residual volume of aqueous extract ~200 mL). This was then extracted 3 times initially with CH<sub>2</sub>Cl<sub>2</sub> (3 × 200 mL) and then 3 times with AcOEt (3 × 200 mL). The AcOEt extract (not dried over magnesium sulfate) was concentrated under reduced pressure to obtain 700 mg of a brown residue. This process was repeated on another nine batches of narcissus bulbs of 500 g each to obtain 7 g of the brown residue. This was resuspended after sonication in a minimum volume of methanol and applied to a silica gel (400 g, 40–63 μm) flash chromatography column (7 cm in diameter), which was eluted with CH<sub>2</sub>Cl<sub>2</sub> (2.5 L) and then CH<sub>2</sub>Cl<sub>2</sub>/MeOH (3 L 9:1 v/v). The relevant product fractions as determined by TLC (*R<sub>f</sub>*: 0.6 using CH<sub>2</sub>Cl<sub>2</sub>/MeOH (8:2 v/v)) were combined and the solvent evaporated to give 1.5 g of a brown solid. This solid was resuspended in a maximum 50 mL of methanol and then sonicated and the resulting solution maintained at ambient temperature for 3 days. The precipitate that formed was then filtered to obtain 550 mg of fine needles of pure narciclasine (**1**). The overall yield was 0.011% starting from fresh bulbs. The product's physical and spectral properties were identical to those previously published.<sup>23,26</sup> (i) mp: 250–252 °C. (ii) TLC *R<sub>f</sub>*: 0.6 (CH<sub>2</sub>Cl<sub>2</sub>/MeOH: 8:2 v/v). (iii) RP-HPLC (C<sub>18</sub>): system 1, *R<sub>t</sub>* = 5.08 min, and purity, 99.9%, and system 5, *R<sub>t</sub>* = 6.15 min and purity: 99.9%. (iv) <sup>1</sup>H NMR (DMSO-*d*<sub>6</sub>): δ 13.25 (s, 1H exchangeable with D<sub>2</sub>O, PhOH), 7.89 (s, 1H exchangeable with D<sub>2</sub>O, NH), 6.86 (s, 1H, PhH), 6.16 (m, 1H, =CH), 6.09 (s, 2H, O–CH<sub>2</sub>–O), 5.19 (m, 2H exchangeable with D<sub>2</sub>O, OH), 5.03 (m, 1H exchangeable with D<sub>2</sub>O, OH), 4.19–3.71 (m, 4H, HC-2, HC-3, HC-4, HC-4a); <sup>13</sup>C NMR: (DMSO-*d*<sub>6</sub>): δ 169.50 (C-6), 152.90 (C-9), 145.39 (C-10b), 133.99 (C-7), 132.68 (C-8), 129.82 (C-10a), 125.28 (C-1), 106.11 (C-6a), 102.64 (C-11), 96.40 (C-10), 72.94 (C-3), 69.41 (C-4), 69.71 (C-2), 53.44 (C-4a) and <sup>1</sup>H-<sup>1</sup>H COSY, HMBC, HMQC, NOESY spectra confirm all hydrogen and carbon attributions. (v) MS (EI): *m/z* 307 (M<sup>+</sup>), 271, 247, 218 and MS (ESI): *m/z* 308 (MH<sup>+</sup>).

**Glycosylated Products 5k and 5l.** Narciclasine 2,3,4-(triacetate) **4** (150 mg, 346 μmol) and 2,3,4,6-tetra-*O*-benzoyl-α-D-glucopyranosyl bromide (455 mg, 690 μmol) were dissolved in extra dry CH<sub>2</sub>Cl<sub>2</sub>. This mixture was stirred and cooled to –78 °C. Allyltrimethylsilane (315 μL, 1972 μmol) and silver trifluoromethane sulfonate (175 mg, 690 μmol) in 5 mL of dry toluene were added. The temperature was slowly allowed to rise to room temperature without removing the cooling bath. After 17 h of reaction, the mixture was filtered through celite and evaporated to a reduced volume. Purification of this crude mixture by silica gel chromatography with cyclohexane/AcOEt (7:3 to 1:1 v/v) gave **5k** as a white solid (143 mg) and **5l** as a white powder (92 mg).

Acetic acid 2,3-diacetoxy-7-*O*-(2',3',4',6'-tetra-*O*-benzoyl-α-D-glucopyranosyl)-6-*oxo*-2,3,4,4a,5,6-hexahydro-[1,3]dioxolo[4,5-*j*]phenanthridin-4-yl ester (**5k**): (i) Yield: 41%. (ii) TLC *R<sub>f</sub>*: 0.43

(CH<sub>2</sub>Cl<sub>2</sub>/MeOH: 96:4 v/v). (iii) <sup>1</sup>H NMR (DMSO-*d*<sub>6</sub>): δ 8.54 (s, 1H, NH), 7.90–7.41 (m, 20H, –OC–PhH), 7.09 (s, 1H, PhH), 6.59 (t, <sup>3</sup>J<sub>3'-4'</sub> = <sup>3</sup>J<sub>3'-2'</sub> = 9.6 Hz, 1H, HC-3'), 6.45 (d, <sup>3</sup>J<sub>1'-2'</sub> = 3.3 Hz, 1H, HC-1'), 6.26 (m, 1H, =CH), 6.10 (s, 1H, O–CH–O), 6.03 (s, 1H, O–CH–O), 5.73 (t, <sup>3</sup>J<sub>4'-3'</sub> = <sup>3</sup>J<sub>4'-5'</sub> = 9.9 Hz, 1H, HC-4'), 5.65 (dd, <sup>3</sup>J<sub>2'-3'</sub> = 10.2 Hz, <sup>3</sup>J<sub>2'-1'</sub> = 3.9 Hz, 1H, HC-2'), 5.31–5.21 (m, 3H, HC-2, HC-3, HC-5'), 4.99 (m, 1H, HC-4), 4.45–4.38 (m, 3H, HC-4a, H<sub>2</sub>C-6'), 2.09 (s, 3H, CH<sub>3</sub>CO), 2.05 (s, 3H, CH<sub>3</sub>CO), 2.02 (s, 3H, CH<sub>3</sub>CO) and <sup>13</sup>C NMR (DMSO-*d*<sub>6</sub>): δ 169.98 (O=C–O), 169.49 (O=C–O), 169.25 (O=C–O), 165.01–164.80 (4C, O=C–O benzoate), 161.99 (C-6), 151.42 (C-9), 138.73 (C-10b), 137.33 (C-7), 134.89 (C-8), 133.83–133.34 (m, *Ph* benzoate), 132.00 (C-10a), 129.23–128.43 (*Ph* benzoate), 117.59 (C-1), 114.39 (C-6a), 102.44 (C-11), 100.35 (C-1'), 99.57 (C-10), 71.14–62.73 (8C, C-3, C-4, C-2, C-2', C-3', C-4', C-5', C-6'), 49.00 (C-4a), 20.89 (CH<sub>3</sub>CO), 20.51 (CH<sub>3</sub>CO), 20.42 (CH<sub>3</sub>CO). (iv) MS (ESI): *m/z* 1034 (MNa<sup>+</sup>) 1012 (MH<sup>+</sup>), 579.

2,3,4-Trihydroxy-7-(3,4,5-trihydroxy-6-hydroxymethyl-tetrahydro-pyran-2-yloxy)-3,4,4a,5-tetrahydro-2H-[1,3]dioxolo[4,5-*f*]phenanthridin-6-one (**7k**): Compound **5k** (113 mg, 112 μmol) and K<sub>2</sub>CO<sub>3</sub> (20 mg, 144 μmol) were added to MeOH (15 mL) containing two drops of water and stirred at ambient temperature for 16 h. The solvent was removed under vacuum and the residue purified by column chromatography using (CH<sub>2</sub>Cl<sub>2</sub>/MeOH/H<sub>2</sub>O 70:30:5 v/v/v) to give **7k** as a white solid (44 mg): (i) Yield: 84%. (ii) TLC *R*<sub>f</sub>: 0.62 (CH<sub>2</sub>Cl<sub>2</sub>/MeOH/H<sub>2</sub>O 70:30:5 v/v/v). (iii) RP-HPLC (C<sub>18</sub>): system 3, *R*<sub>t</sub> = 10.28 min and purity, 98.3% and system 6, *R*<sub>t</sub> = 9.12 min and purity, 99.7%. (iv) <sup>1</sup>H NMR (DMSO-*d*<sub>6</sub>): δ 7.72 (s, 1H, NH), 7.13 (s, 1H, HC-10), 6.17 (m, 1H, =CH), 6.11 (s, 1H, O–CH–O), 6.08 (s, 1H, O–CH–O), 5.47 (m, 1H, OH), 5.25 (d, <sup>3</sup>J<sub>1'-2'</sub> = 3.6 Hz, 1H, HC-1'), 5.02 (m, 2H, OH), 4.41–3.10 (m, 14H, OH, CH<sub>2</sub>, HC-2', HC-3', HC-4', HC-5', HC-2, HC-3, HC-4, HC-4a); <sup>13</sup>C NMR (DMSO-*d*<sub>6</sub>): δ 163.36 (C-6), 151.42 (C-9), 141.36 (C-10b), 140.12 (C-7), 133.93 (C-8), 130.69 (C-10a), 124.25 (C-1), 114.33 (C-6a), 103.02, 102.24, 100.50 (C-1', C-10, C-11), 74.03, 73.77, 72.34, 71.70, 69.05, 68.92, 68.80 (C-2', C-3', C-4', C-5', C-3, C-4, C-2), 60.16 (CH<sub>2</sub>-O), 52.70 (C-4a). (v) MS (ESI) *m/z* 492 (MNa<sup>+</sup>).

**Pharmacology. In Vitro Pharmacology: Cell Lines.** Human cancer cell lines were obtained from the American Type Culture Collection (ATCC, Manassas, VA), the European Collection of Cell Culture (ECACC, Salisbury, UK), and the Deutsche Sammlung von Mikroorganismen und Zellkulturen (DSMZ, Braunschweig, Germany). The code numbers and histological types of all the cell lines used in the current study are detailed in Table 2. The GL-19 GBM primoculture is part of a collection of several hundred GBM primocultures established within the Department of Neurosurgery of the Wagner Jauregg Hospital (Linz, Austria).

**Biological, Biochemical and Molecular Biology Related Experiments.** The effects of narciclasine and its derivatives on: (1) The overall growth level of human cancer cell lines was determined using the colorimetric MTT (3-[4,5-dimethylthiazol-2-yl]-diphenyl tetrazolium bromide, Sigma, Belgium) assay.<sup>9,10,20,21</sup> (2) Cell proliferation (mitosis) and cell migration were determined by means of computer-assisted phase contrast microscopy.<sup>8–10,21,22</sup> (3) The actin cytoskeleton organization was determined by means of computer-assisted fluorescence microscopy.<sup>21</sup> (4) Apoptosis and necrosis were determined by means of flow cytometry as detailed elsewhere.<sup>33</sup>

**In Vivo Testing.** All the in vivo experiments described in the present study were performed on the basis of authorization no. LA1230509 of the Animal Ethics Committee of the Belgian Federal Department of Health, Nutritional Safety, and the Environment.

**In Vivo Toxicology Study of Narciclasine (1) in Rats.** The study was performed according to ICH Harmonized Tripartite Guidelines: Nonclinical Safety Studies for the Conduct of Human Clinical Trials for Pharmaceuticals (16 July 1997) and undertaken at Notox B.V. (s'-Hertogenbosch, The Netherlands: Notox project 487389 and Unibioscreen reference no. 4818-2-5-001).

**In Vivo Evaluation of Anti-Tumor Activity.** The details of each experiment are provided in the Discussion Section and also

form part of the legends to the figures. The rest of the information is provided in the Supporting Information. The potential survival gain obtained using narciclasine and its derivatives was evaluated by means of survival curve analysis.<sup>9,10,29,31,39</sup>

**In Vivo Determination of Narciclasine (1) and its Prodrug (7k) Plasma Concentrations.** The experimental protocols are detailed in the Supporting Information.

**Statistical Analyses.** Statistical comparison of control and treated groups was initially undertaken with the Kruskal–Wallis test (a nonparametric one-way analysis of variance). Where this revealed significant differences, the Dunn multiple comparison procedure (2-sided test) was applied. However, this was adapted to the special case of comparing treatment and control groups in which only (*k* – 1) comparisons were undertaken among the *k* groups tested by the Kruskal–Wallis test (instead of the possible *k*(*k* – 1)/2 comparisons considered in the general procedure). The levels of statistical significance associated with the %*T/C* (test/control) survival indices were determined by using Gehan's generalized Wilcoxon test. The correlation between numerical variables was analyzed by means of the nonparametric Spearman correlation test. All these statistical analyses were carried out using Statistica (Statsoft, Tulsa, OK).

**Acknowledgment.** This work was partially supported by grants awarded by the “Région de Bruxelles-Capitale” (Brussels, Belgium) and by the Fonds Yvonne Boël (Brussels, Belgium). We greatly thank Jean-François Gaussin, Stéphanie Thomas, Gwenaël Dielie, Lise Włodarczak, and Gentiane Simon for their excellent technical assistance.

**Supporting Information Available:** The results of the analysis of all compounds synthesized and evaluated in this study with the exception of **1**, **5k**, and **7k** (HPLC, <sup>1</sup>H NMR, <sup>13</sup>C NMR, and mass spectra). This material is available free of charge via the Internet at <http://pubs.acs.org>.

## References

- (1) Lefranc, F.; Brotchi, J.; Kiss, R. Possible future issues in the treatment of glioblastomas: special emphasis on cell migration and the resistance of migrating glioblastoma cells to apoptosis. *J. Clin. Oncol.* **2005**, *23*, 2411–2422.
- (2) Eberle, J.; Kurbanov, B. M.; Hossini, A. M.; Trefzer, U.; Fecker, L. F. Overcoming apoptosis deficiency of melanoma—hope for new therapeutic approaches. *Drug Resist. Updates* **2007**, *10*, 218–234.
- (3) Malthaner, R. A.; Collin, S.; Fenlon, D. *Preoperative Chemotherapy for Resectable Thoracic Esophageal Cancer. Review, The Cochrane Library*; John Wiley & Sons: New York, 2007; pp 1–34.
- (4) Giovannetti, E.; Mey, V.; Nannizzi, S.; Pasqualetti, G.; Del Tacca, M.; Danesi, R. Pharmacogenetics of anticancer drug sensitivity in pancreatic cancer. *Mol. Cancer Ther.* **2006**, *5*, 1387–1395.
- (5) Uzzo, R. G.; Haas, N. B.; Crispin, P. L.; Kolenko, V. M. Mechanisms of apoptosis resistance and treatment strategies to overcome them in hormone-refractory prostate cancer. *Cancer* **2008**, *112*, 1660–1671.
- (6) Shivapurkar, N.; Reddy, J.; Chaudhary, P. M.; Gazdar, A. F. Apoptosis and lung cancer: a review. *J. Cell Biochem.* **2003**, *88*, 885–898.
- (7) Lefranc, F.; Facchini, V.; Kiss, R. Proapoptotic drugs: a novel means to combat apoptosis-resistant cancers, with a special emphasis on glioblastomas. *Oncologist* **2007**, *12*, 1395–1403.
- (8) Lefranc, F.; James, S.; Camby, I.; Gaussin, J. F.; Darro, F.; Brotchi, J.; Gabius, H. J.; Kiss, R. Combined cimetidine and temozolomide, compared with temozolomide alone: significant increases in survival in nude mice bearing U373 human glioblastoma multiforme orthotopic xenografts. *J. Neurosurg.* **2005**, *102*, 706–714.
- (9) Joseph, B.; Darro, F.; Behard, A.; Lesur, B.; Collignon, F.; Decaestecker, C.; Frydman, A.; Guillaumet, G.; Kiss, R. 3-Aryl-2-quinolone derivatives: synthesis and characterization of in vitro and in vivo antitumor effects with emphasis on a new therapeutic target connected with cell migration. *J. Med. Chem.* **2002**, *45*, 2543–2555.
- (10) Ingrassia, L.; Nshimyumukiza, P.; Dewelle, J.; Lefranc, F.; Włodarczak, L.; Thomas, S.; Dielie, G.; Chiron, C.; Zedde, C.; Tisnès, P.; van Soest, R.; Braeckman, J. C.; Darro, F.; Kiss, R. A lactosylated steroid contributes in vivo therapeutic benefits in experimental models of mouse lymphoma and human glioblastoma. *J. Med. Chem.* **2006**, *49*, 1800–1807.
- (11) Koehn, F. E.; Carter, G. T. The evolving role of natural products in drug discovery. *Nat. Rev. Drug Discovery* **2005**, *4*, 206–220.

- (12) Newman, D. J.; Cragg, G. M. Natural products as sources of new drugs over the last 25 years. *J. Nat. Prod.* **2007**, *70*, 461–477.
- (13) Mann, J. Natural products in cancer chemotherapy: past, present and future. *Nat. Rev. Cancer* **2002**, *2*, 143–148.
- (14) Altmann, K. H.; Gertsch, J. Anticancer drugs from nature—natural products as a unique source of new microtubule-stabilizing agents. *Nat. Prod. Rep.* **2007**, *24*, 327–357.
- (15) Ingrassia, L.; Lefranc, F.; Mathieu, V.; Darro, F.; Kiss, R. Amaryllidaceae isocarbostryl alkaloids and their derivatives as promising antitumor agents. *Transl. Oncol.* **2008**, *1*, 1–13.
- (16) Kornienko, A.; Evidente, A. Chemistry, biology, and medicinal potential of narciclasine and its congeners. *Chem. Rev.* **2008**, *108*, 1982–2014.
- (17) Ceriotti, G. Narciclasine: an antimetabolic substance from narcissus bulbs. *Nature* **1967**, *213*, 595–596.
- (18) Carrasco, L.; Fresno, M.; Vazquez, D. Narciclasine: an antitumoral alkaloid which blocks peptide bond formation by eukaryotic ribosomes. *FEBS Lett.* **1975**, *52*, 236–239.
- (19) MacLachlan, A.; Kekre, N.; McNulty, J.; Pandey, S. Pancreatistatin: a natural anticancer compound that targets mitochondria specifically in cancer cells to induce apoptosis. *Apoptosis* **2005**, *10*, 619–630.
- (20) Dumont, P.; Ingrassia, L.; Rouzeau, S.; Ribaucour, F.; Thomas, S.; Roland, I.; Darro, F.; Lefranc, F.; Kiss, R. The Amaryllidaceae isocarbostryl narciclasine induces apoptosis by activation of the death receptor and/or mitochondrial pathways in cancer cells but not in normal fibroblasts. *Neoplasia* **2007**, *9*, 766–776.
- (21) Hayot, C.; Debeir, O.; Van Ham, P.; Van Damme, M.; Kiss, R.; Decaestecker, C. Characterization of the activities of actin-affecting drugs on tumor cell migration. *Toxicol. Appl. Pharmacol.* **2006**, *211*, 30–40.
- (22) Decaestecker, C.; Debeir, O.; Van Ham, P.; Kiss, R. Can anti-migratory drugs be screened in vitro? A review of 2D and 3D assays for the quantitative analysis of cell migration. *Med. Res. Rev.* **2007**, *27*, 149–176.
- (23) Kireev, A. S.; Nadein, O. N.; Agustin, V. J.; Bush, N. E.; Evidente, A.; Manpadi, M.; Ogasawara, M. A.; Rastogi, S. K.; Rogelj, S.; Shors, S. T.; Kornienko, A. Synthesis and biological evaluation of aromatic analogues of condritol F, L-chiro-inositol, and dihydrocondritol F structurally related to the Amaryllidaceae anticancer constituents. *J. Org. Chem.* **2006**, *71*, 5694–5707.
- (24) Nadein, O. N.; Kornienko, A. An approach to pancreatistatins via ring-closing metathesis: efficient synthesis of novel 1-aryl-1-deoxycondritols F. *Org. Lett.* **2004**, *6*, 831–834.
- (25) Ingrassia, L.; Wlodarczyk, L.; Thomas, S.; Van Quaquebeke, E.; Van den Hove, L.; Kiss, R.; Darro, F. New isocarbostryl alkaloid derivatives. Patent WO2008043846, 2008.
- (26) Evidente, A. Narciclasine <sup>1</sup>H- and <sup>13</sup>C-NMR data and a new improved method of preparation. *Planta Med.* **1991**, *57*, 293–294.
- (27) Pettit, G. R.; Melody, N.; Herald, D. L. Antineoplastic agents: 450. Synthesis of (+)-pancratistatin from (+)-narciclasine as relay. *J. Org. Chem.* **2001**, *66*, 2583–2587.
- (28) Pettit, G. R.; Orr, B.; Ducki, S. Synthesis of pancreatistatin prodrugs. WIPO patent WO02085848, October 31, 2002.
- (29) Branle, F.; Lefranc, F.; Camby, I.; Jeuken, J.; Geurts-Moespot, A.; Sprenger, S.; Sweep, F.; Kiss, R.; Salmon, I. Evaluation of the efficiency of chemotherapy in vivo orthotopic models of human glioma cells with and without 1p19 deletions and in C6 rat orthotopic allografts serving for the evaluation of surgery combined with chemotherapy. *Cancer* **2002**, *95*, 641–655.
- (30) Belot, N.; Rorive, S.; Doyen, I.; Lefranc, F.; Bruyneel, E.; Dedecker, R.; Micik, S.; Brotchi, J.; Decaestecker, C.; Salmon, I.; Kiss, R.; Camby, I. Molecular characterization of cell substratum attachments in human glial tumors relates to prognostic features. *Glia* **2001**, *36*, 375–390.
- (31) Roos, W. P.; Batista, L. F.; Naumann, S. C.; Wick, W.; Weller, M.; Menck, C. F.; Kaina, B. Apoptosis in malignant glioma cells triggered by the temozolomide-induced DNA lesion O6-methylguanine. *Oncogene* **2007**, *26*, 186–197.
- (32) Mathieu, A.; Rummelink, M.; D'Haene, N.; Penant, S.; Gaussin, J. F.; Van Ginckel, R.; Darro, F.; Kiss, R.; Salmon, I. Development of a chemoresistant orthotopic human non-small cell lung carcinoma model in nude mice. *Cancer* **2004**, *101*, 1908–1918.
- (33) Mijatovic, T.; Mathieu, V.; Gaussin, J. F.; De Neve, N.; Ribaucour, F.; Van Quaquebeke, E.; Dumont, P.; Darro, F.; Kiss, R. Cardenolide-induced lysosomal membrane permeabilization demonstrates therapeutic benefits in experimental human non-small cell lung cancers. *Neoplasia* **2006**, *8*, 402–412.
- (34) Mijatovic, T.; Op De Beeck, A.; Van Quaquebeke, E.; Dewelle, J.; Darro, F.; de Launoit, Y.; Kiss, R. The cardenolide UNBS1450 is able to deactivate nuclear factor kappaB-mediated cytoprotective effects in human non-small cell lung cancer cells. *Mol. Cancer Ther.* **2006**, *5*, 391–399.
- (35) Pettit, G. R.; Eastham, S. A.; Melody, N.; Orr, B.; Herald, D. L.; McGregor, J.; Knight, J. C.; Doubek, D. L.; Pettit III, G. R.; Garner, L. C.; Bell, J. A. Isolation and structural modification of 7-deoxynarciclasine and 7-deoxy-trans-dihydranarciclasine. *J. Nat. Prod.* **2006**, *69*, 7–13.
- (36) McNulty, J.; Mao, J.; Gibe, R.; Mo, R.; Wolf, S.; Pettit, G. R.; Herald, D. L.; Boyd, M. R. Studies directed towards the refinement of the pancreatistatin cytotoxic pharmacophore. *Bioorg. Med. Chem. Lett.* **2001**, *11*, 169–172.
- (37) Rinner, U.; Hillebrenner, H. L.; Adams, D. R.; Hudlicky, T.; Pettit, G. R. Synthesis and biological activity of some structural modifications of pancreatistatin. *Bioorg. Med. Chem. Lett.* **2004**, *14*, 2911–2915.
- (38) Abou-Donia, A. H.; De Giulio, A.; Evidente, A.; Gaber, M.; Habib, A.-A.; Lanzetta, R.; Seif El Din, A. Narciclasine-4-O-β-D-glucopyranoside, a glucosyloxy amidic phenanthridone derivative from *Pancreatium maritimum*. *Phytochemistry* **1991**, *30*, 3445–3448.
- (39) Van Quaquebeke, E.; Mahieu, T.; Dumont, P.; Dewelle, J.; Ribaucour, F.; Simon, G.; Sauvage, S.; Gaussin, J. F.; Tuti, J.; El Yazidi, M.; Van Vynckt, F.; Mijatovic, T.; Lefranc, F.; Darro, F.; Kiss, R. 2,2,2-Trichloro-N-((2-[2-(dimethylamino)ethyl]-1,3-dihydro-1H-benzo[de]isoquinolin-5yl)carbamoyl)acetamide (UNBS3157), a novel nonhematotoxic naphthalimide derivative with potent antitumor activity. *J. Med. Chem.* **2007**, *50*, 4122–4134.
- (40) Le Mercier, M.; Lefranc, F.; Mijatovic, T.; Debeir, O.; Haibe-Kains, B.; Bontempi, G.; Decaestecker, C.; Kiss, R.; Mathieu, V. Evidence of galectin-1 involvement in glioma chemoresistance. *Toxicol. Appl. Pharmacol.* **2008**, *229*, 172–183.
- (41) Le Mercier, M.; Mathieu, V.; Haibe-Kains, B.; Bontempi, G.; Mijatovic, T.; Decaestecker, C.; Kiss, R.; Lefranc, F. Knocking down galectin-1 in human Hs683 glioblastoma cells impairs both angiogenesis through ORP150 depletion and endoplasmic reticulum stress responses. *J. Neuropathol. Exp. Neurol.* **2008**, *67*, 456–469.
- (42) Berger, W.; Spiegl-Kreinecker, S.; Buchroither, J.; Elbling, L.; Pirker, C.; Fischer, J.; Micksche, M. Overexpression of the human major vault protein in astrocytic brain tumor cells. *Int. J. Cancer* **2001**, *94*, 377–382.
- (43) Griffin, C.; Sharda, N.; Sood, D.; Nair, J.; McNulty, J.; Pandey, S. Selective cytotoxicity of pancreatistatin-related natural Amaryllidaceae alkaloids: evaluation of the activity of two new compounds. *Cancer Cell Int.* **2007**, *7*, 10.
- (44) Ghosh, M.; Song, X.; Mouneimne, G.; Sidani, M.; Lawrence, D. S.; Condeelis, J. S. Cofilin promotes actin polymerization and defines the direction of cell motility. *Science* **2004**, *304*, 743–746.
- (45) Yap, C. T.; Simpson, T. I.; Pratt, T.; Price, D. J.; Maciver, S. K. The motility of glioblastoma tumour cells is modulated by intracellular cofilin expression in a concentration-dependent manner. *Cell Motil Cytoskeleton* **2005**, *60*, 153–165.
- (46) Jansen, R. P. RNA-cytoskeletal associations. *FASEB J.* **1999**, *13*, 455–466.
- (47) Mégalizzi, V.; Mathieu, V.; Mijatovic, T.; Gailly, P.; Debeir, O.; De Neve, N.; Van Damme, M.; Bontempi, G.; Haibe-Kains, B.; Decaestecker, C.; Kondo, Y.; Kiss, R.; Lefranc, F. 4-IBP, a sigma1 receptor agonist, decreases the migration of human cancer cells, including glioblastoma cells, in vitro and sensitizes them in vitro and in vivo to cytotoxic insults of proapoptotic and proautophagic drugs. *Neoplasia* **2007**, *9*, 358–369.

JM8013585